


Graphene oxide significantly inhibits cell growth at sublethal concentrations by causing extracellular iron deficiency

Qilin Yu, Bing Zhang, Jianrong Li, Tingting Du, Xiao Yi, Mingchun Li, Wei Chen & Pedro J. J. Alvarez



To cite this article: Qilin Yu, Bing Zhang, Jianrong Li, Tingting Du, Xiao Yi, Mingchun Li, Wei Chen & Pedro J. J. Alvarez (2017): Graphene oxide significantly inhibits cell growth at sublethal concentrations by causing extracellular iron deficiency, *Nanotoxicology*, DOI: [10.1080/17435390.2017.1398357](https://doi.org/10.1080/17435390.2017.1398357)

To link to this article: <http://dx.doi.org/10.1080/17435390.2017.1398357>

 View supplementary material 

 Published online: 09 Nov 2017.

 Submit your article to this journal 

 View related articles 

 View Crossmark data 

ORIGINAL ARTICLE



Graphene oxide significantly inhibits cell growth at sublethal concentrations by causing extracellular iron deficiency

Qilin Yu^a, Bing Zhang^a, Jianrong Li^a, Tingting Du^b, Xiao Yi^a, Mingchun Li^a, Wei Chen^b and Pedro J. J. Alvarez^c

^aKey Laboratory of Molecular Microbiology and Technology, Ministry of Education, College of Life Science, Nankai University, Tianjin, China; ^bCollege of Environmental Science and Engineering, Tianjin Key Laboratory of Environmental Remediation and Pollution Control, Nankai University, Tianjin, China; ^cDepartment of Civil and Environmental Engineering, Rice University, Houston, TX, USA

ABSTRACT

Graphene oxide (GO)-based materials are increasingly being used in medical materials and consumer products. However, their sublethal effects on biological systems are poorly understood. Here, we report that GO (at 10 to 160 mg/L) induced significant inhibitory effects on the growth of different unicellular organisms, including eukaryotes (i.e. *Saccharomyces cerevisiae*, *Candida albicans*, and *Komagataella pastoris*) and prokaryotes (*Pseudomonas fluorescens*). Growth inhibition could not be explained by commonly reported cytotoxicity mechanisms such as plasma membrane damage or oxidative stress. Based on transcriptomic analysis and measurement of extra- and intracellular iron concentrations, we show that the inhibitory effect of GO was mainly attributable to iron deficiency caused by binding to the O-functional groups of GO, which sequestered iron and disrupted iron-related physiological and metabolic processes. This inhibitory mechanism was corroborated with supplementary experiments, where adding bathophenanthroline disulfonate—an iron chelating agent—to the culture medium exerted similar inhibition, whereas removing surface O-functional groups of GO decreased iron sequestration and significantly alleviated the inhibitory effect. These findings highlight a potential indirect detrimental effect of nanomaterials (i.e. scavenging of critical nutrients), and encourage research on potential biomedical applications of GO-based materials to sequester iron and enhance treatment of iron-dependent diseases such as cancer and some pathogenic infections.

ARTICLE HISTORY

Received 20 May 2017
Revised 25 September 2017
Accepted 14 October 2017

KEYWORDS

Graphene oxide; iron deficiency; transcription profiling; sublethal concentration; growth inhibition

Introduction

Graphene oxide (GO) and its derivatives are an emerging class of carbon nanomaterials that possess extraordinary electronic, mechanical, optical and thermal properties, and have shown great promise in many potential applications (Buriak and Toro, 2015; Compton and Nguyen, 2010; Zhu et al., 2010). Furthermore, GO materials have been considered as an excellent candidate for a number of biomedical applications, ranging from gene and drug delivery to bio-imaging and bio-sensing (Chung et al., 2013; Liang et al., 2015). The increasing production, use, and accidental or incidental release of these materials call for improved understanding of their potential human health and ecological effects (Seabra et al., 2014; Turco et al., 2011). Because released GO-based materials would likely reach

biological systems at relatively low concentrations (Gottschalk, Sun, and Nowack 2013; Mueller and Nowack, 2008), there is a particular need to discern sublethal effects. This would inform risk assessment and also enable their benign use in medical practices.

Cytotoxicity of GO has been previously reported (Chatterjee et al., 2017; Chen et al., 2016; Ema et al., 2016). The sharp edges and thin-film structure of GO may cause plasma membrane damage (Carpio et al., 2012; Mangadlao et al., 2015; Perreault et al., 2015; Zou et al., 2016). GO can also lead to oxidative stress regardless of the participation of induced reactive oxygen species (ROS) (Li et al., 2014; Liu et al., 2011), as well as interfere with biochemical functions by interacting with intracellular components such as proteins and deoxyribonucleic acid

CONTACT Mingchun Li ✉ nklimingchun@163.com 📧 College of Life Science, Nankai University, Wei Jin Rd. 94, Tianjin 300071, China; Wei Chen ✉ chenwei@nankai.edu.cn 📧 College of Environmental Science and Engineering, Nankai University, 38 Tongyan Rd., Tianjin 300350, China
📎 Supplemental data for this article can be accessed [here](#).

(DNA) (Feng et al., 2016; Frost et al., 2016). These effects often result in cell apoptosis and necrosis (Seabra et al., 2014; Bianco, 2013; Qu et al., 2013). Most of the previous studies on GO cytotoxicity focused on exposure of organisms to lethal-concentrations of GO. Only one study investigated the effect of GO at sublethal concentrations, and showed that GO may promote the growth of both bacteria and mammalian cells, even though the specific mechanisms were not discussed (Ruiz et al., 2011). To date, no studies have reported detrimental biological effects of GO at sublethal concentrations.

Various nanomaterials (e.g. carbon nanotubes and CeO₂ nanoparticles) can adsorb and decrease the bioavailability of different nutrients, such as folate, amino acids, proteins, phosphate, and metal ions (Guo et al., 2008; Hoecke et al., 2009; Hernandez-Viezas et al., 2016; Lowry et al., 2012; Ma et al., 2015). Accordingly, even at sublethal concentrations, nanomaterials may hinder biological systems by depleting extracellular nutrients that are essential for cell growth. Thus far, only one study has reported this issue – it attributed the inhibitory effect of carbon nanotubes to their adsorption and extracellular depletion of folate (Guo et al., 2008). GO is rich in surface O-functional groups (Dreyer et al., 2010), and can interact strongly with many different nutrients (e.g. metal ions, amino acids, and vitamins). In particular, the carboxyl and phenolic groups of GO are strong metal-complexing moieties (Gao et al., 2017a; Ren et al., 2014, 2016; Sitko et al., 2013; Sun et al., 2013; Zhao et al., 2011), and can interact strongly with certain divalent and trivalent cations (e.g. Fe³⁺/Fe²⁺, Cu²⁺, Zn²⁺, Mn²⁺, and Ca²⁺) in both extracellular and intracellular environments.

This study investigated how sublethal exposure to GO affects cell growth. We postulated that strong binding of essential elements (e.g. iron) by GO may interfere with their cellular uptake, resulting in significant negative effects on cell growth and impaired metabolism. Four types of unicellular organisms, including eukaryotic and prokaryotic cells (i.e. *Saccharomyces cerevisiae*, *Candida albicans*, *Komagataella pastoris*, and *Pseudomonas fluorescens*) were tested. Cell counting and propidium iodide (PI) staining were used to quantify effects on cell growth at sublethal concentrations. ROS accumulation, endocytosis-induced intracellular dysfunction,

and transcription profiling analyses were also conducted to understand the primary inhibitory mechanisms. Additional confirmatory experiments were conducted to control the bioavailable iron concentration, by using an iron chelating agent and a NaBH₄-reduced GO (rGO). The physiological effects of iron deficiency were corroborated by inhibited adenosine triphosphate (ATP) production and aconitase activity.

Materials and methods

Preparation and characterization of GO and rGO

The GO material used in this study was synthesized using the modified Hummer's method (Hummers and Offeman, 1958). The rGO was prepared by reducing GO with NaBH₄ in a Teflon-lined stainless steel autoclave (Shen et al., 2009). GO and rGO were characterized by atomic force microscopy (AFM, NT-MDT, NTEGRA Prima, Russia), Raman spectroscopy (Renishaw, inVia, UK), Fourier transformed infrared spectra (FT-IR, Bio-rad, FTS6000, Hercules, CA, USA), and X-ray photoelectron spectroscopy (XPS, Kratos Analytical Ltd., Axis Ultra DLD, UK).

The key physicochemical properties of GO are shown in Figure 1. AFM images show that GO had lateral dimensions of 100–1000 nm, and thickness of approximately 1 nm (Figure 1(A)). The Raman spectrum shows the typical G band at ~1580 cm⁻¹, D band at ~1350 cm⁻¹, and 2D band at ~2700 cm⁻¹ (Figure 1(B)), consistent with the literature (Zhao et al., 2011; Valles et al., 2008). The XPS spectrum exhibits strong C KLL, O KLL, O1s, and C1s bands, indicating a high surface O content (30.15%). The C1s spectrum shows the existence of C–O (286.2 eV, 26.38%), C=O (287.8 eV, 16.88%) and O–C=O (289.0 eV, 3.36%) surface functional groups (Figure 1(C)) (Zhao et al., 2011; Waltman, Pacansky, and Bates 1993). FT-IR analysis further confirms that GO contained surface O-functional groups, including C=O (1725 cm⁻¹) and C–O (1161 cm⁻¹ and 1059 cm⁻¹) (Figure 1(D)). The XPS data of rGO show that rGO had much lower surface O-content (11.67%), as the majority of the O-containing groups was removed during reduction (Fig. S1).

Growth inhibition experiments

Stock suspensions of GO and rGO (10,000 mg/L) were prepared in yeast extract–peptone–dextrose

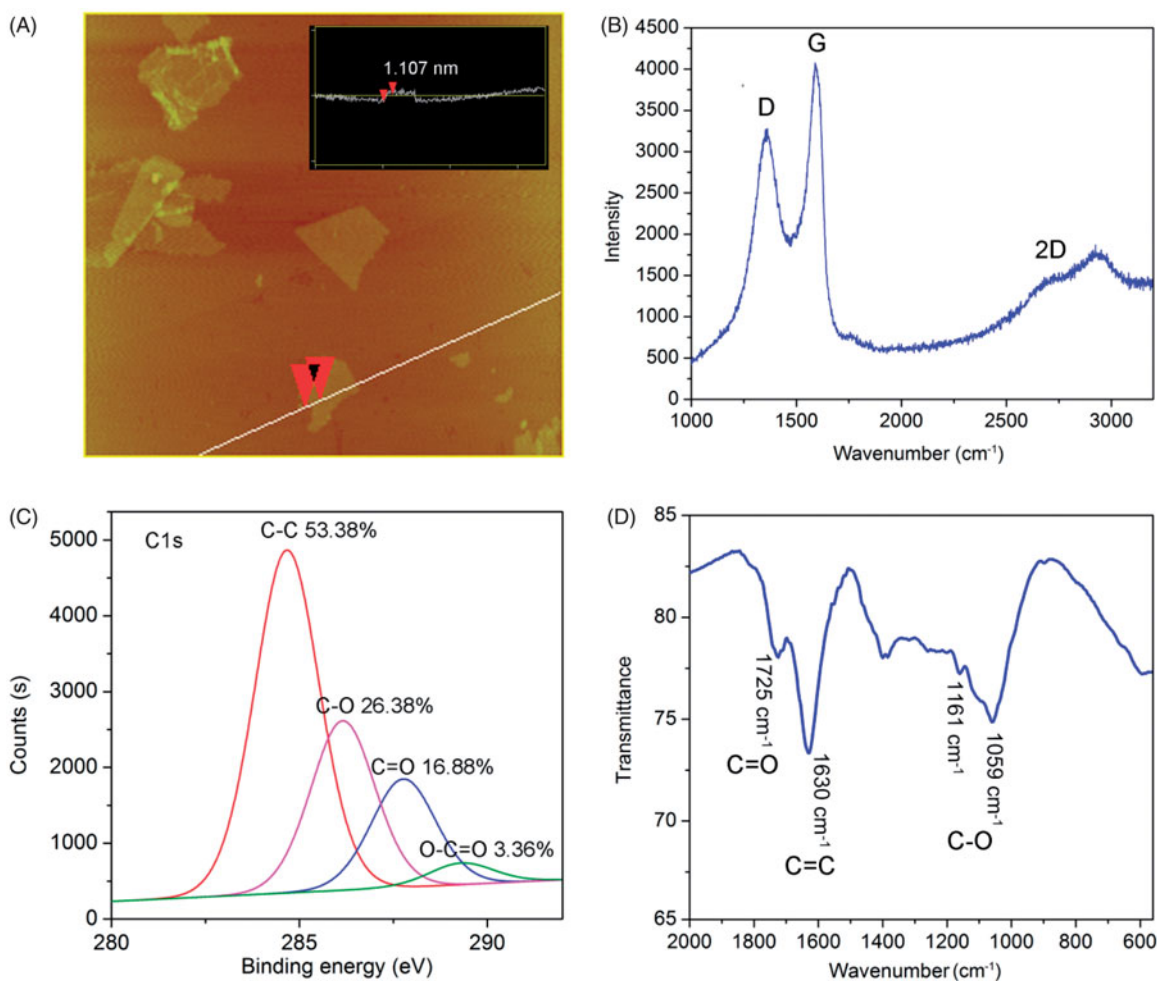


Figure 1. Characterization of as-synthesized GO. (A) AFM image. (B) Raman spectrum. (C) XPS C1s spectrum. (D) FT-IR spectrum.

(YPD) medium (1% yeast extract, 2% peptone, 2% glucose). The stock suspensions were sonicated for 30 min (AS3120, Autoscience, China) before use. Growth inhibition by GO was tested in 20-mL glass tubes. For the concentration-dependent inhibition assay, overnight-cultured *S. cerevisiae* INVSc1 cells (Invitrogen, Carlsbad, CA, USA) were suspended in fresh YPD medium ($OD_{600} = 0.1$) containing GO at varied concentrations (0, 10, 20, 40, 80, 160, 320, and 640 mg/L). Although these values might be relatively high compared to other nanomaterial concentrations predicted by volume-averaged calculations at the regional scale (which typically suggest sub-ppb levels in aquatic systems (Gottschalk, Sun, and Nowack 2013; Mueller and Nowack, 2008)), they are relatively low for therapeutic and antimicrobial applications (Perreault et al., 2015; Liu et al., 2011; Wu et al., 2017). Furthermore, some nanomaterial concentrations near a point of release (e.g. wastewater treatment plant effluents) can easily reach

10s of ppm (Westerhoff et al., 2011; Kiser et al., 2009). Therefore, it is meaningful to investigate the biological effects of GO at the tested concentrations.

The tubes were cultured by shaking at 30 °C for 24 h (or 48 h for longer-term exposure). Then, cells in each tube were counted with hemocytometers, and the percent of growth was calculated as the cell number of each group divided by that of the control (cells receiving no GO treatment) $\times 100$. To determine the effects of Fe^{3+} and the iron chelator bathophenanthroline disulfonate (BPS, Sigma, St. Louis, MO, USA) on the inhibitory effect of GO, the yeast cells were cultured in the medium amended with 1 mM $FeCl_3$ or 200 μ M BPS. To determine the effect of ROS scavengers on the toxicity of GO, the yeast cells were cultured in the medium containing 5 mM N-acetyl-L-cysteine (NAC, Sigma) or 5 mM glutathione (GSH, BBI, China). In the endocytosis inhibition test, the yeast cells were cultured in the

medium containing 0.2 mg/L filipin (Sigma) or 2 μ M cytochalasin D (Cyt D, Invitrogen). Growth inhibition tests of GO to other microbes were described in Supporting Information (SI).

Cell damage assays

To determine cell damage under GO treatment, the yeast cells were treated with GO for 24 h as described above. The cells were harvested, washed with PBS and stained with PI (prepared in double-distilled water, final concentration of 5 mg/L, Sigma) for 5 min to assess damage to the plasma membrane (Bulcke, Thiel, and Dringen, 2014). Both the PI-positive cells (dead cells) and the total cells were observed using a fluorescence microscope (BX53, Olympus, Japan). At least 20 fields were measured. Cell damage was also observed using transmission electron microscopy (TEM) as described in SI.

Transcription profiling analysis

To investigate the transcription profiling under GO treatment, the yeast cells were cultured in YPD medium or the medium containing 160 mg/L GO at 30 °C for 24 h, and then harvested for ribonucleic acid (RNA) extraction. Total RNAs were extracted from the treated cells using the hot phenol method (Shirzadegan, Christie, and Seemann 1991). The quality and quantity of the total RNAs were analyzed using a NanoDrop 2000 spectrophotometer (Thermo Scientific, Waltham, MA, USA) and gel electrophoresis. RNAs were used to generate double-stranded cDNA using the SMARTTM cDNA Library Construction Kit (Clontech, Mountain View, CA, USA). The obtained cDNAs were then used to construct a 454 library. Roche GS-FLX 454 pyrosequencing was carried out using Illumina HiSeqTM 2000 (Oebiotech Company, China). Gene annotations were retrieved from *S. cerevisiae* genome browser (www.yeastgenome.org). Assignment of Gene Ontology and Kyoto Encyclopedia of Genes and Genomes (KEGG) terms was based on Joint Genome Institute (JGI) annotations. Enrichment of differentially regulated genes in Gene Ontology and KEGG was determined using GOSec (Gou, Onnis-Hayden, and Gu, 2010). The results of transcription profiling analysis were confirmed by the real-time polymerase chain reaction (RT-PCR) as described in SI.

Biochemical analyses

ROS levels in the GO-treated cells were assessed using the oxidant-sensitive agent 2',7'-dichlorofluorescein diacetate (DCFH-DA) (Liu et al., 2010). The yeast cells were treated with different concentrations of GO for 24 h, washed twice with PBS buffer, and stained with DCFH-DA (dissolved in PBS buffer, final concentration of 10 mg/L) at 30 °C for 50 min. The stained cells were washed again with PBS buffer, and observed with a fluorescence microscope (BX53, Olympus, Japan) equipped with the GFP filter set. The DCF fluorescence-positive cells (ROS-accumulating cells), and the total cells were counted in each field. At least 30 fields were observed.

ATP contents in the yeast cells were determined based on the ATP-dependent luciferase (Lundin, 1999). The yeast cells were treated by GO (160 mg/L), Fe³⁺, and BPS in YPD medium for 24 h, harvested, suspended in 0.05 M Tris-HCl (pH 7.6) and broken by alternately vortexing and freezing with liquid nitrogen. The lysates were centrifuged at 12,000 rpm for 10 min, and the supernatants were used for ATP assay. ATP contents in the supernatants were detected using an ATP analysis Kit (Beyotime Biotech., China). The protein contents in the supernatants were also determined using the Coomassie brilliant blue agent.

Aconitase activity was assayed by detecting reduced nicotinamide adenine dinucleotide phosphate (NADPH) production coupled with citrate-isocitrate- α -ketoglutaric acid conversion. Aconitase is an important iron-sulfur protein, and its activity reflects iron-dependent mitochondrial function (Beinert, Kennedy, and Stout 1996). The treated yeast cells were harvested and broken as described in ATP assay, obtaining the protein extracts. Aconitase activity of the protein extracts was determined as described previously (Xu et al., 2014).

Iron measurement

To detect extracellular and intracellular iron concentrations, the cultures were centrifuged at 35,000 rpm (OptimaTM LE-80 K, Eppendorf, Hauppauge, NY, USA) for 60 min. Then, both the supernatant and the washed cells were digested with 33% HNO₃, and the iron concentrations were analyzed using an

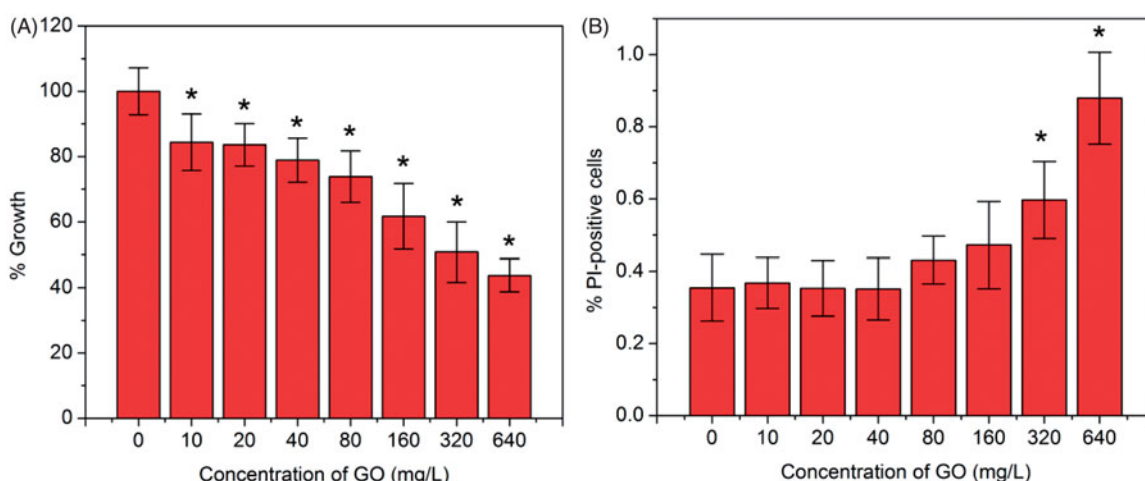


Figure 2. GO treatment significantly inhibits the growth of yeast cells but does not cause noticeable cell death. (A) Growth inhibition. The yeast cells were cultured in YPD medium containing the indicated concentrations of GO for 24 h. The cells were then counted with hemocytometers, and growth (% Growth) was normalized to that of the control. (B) Cell damage. The GO-treated yeast cells were harvested and stained with PI. The percent of PI-positive cells (dead cells) were determined using fluorescence microscopy. Values represent mean \pm SD. * indicates statistical difference between the treatment groups and the control group ($p < 0.05$).

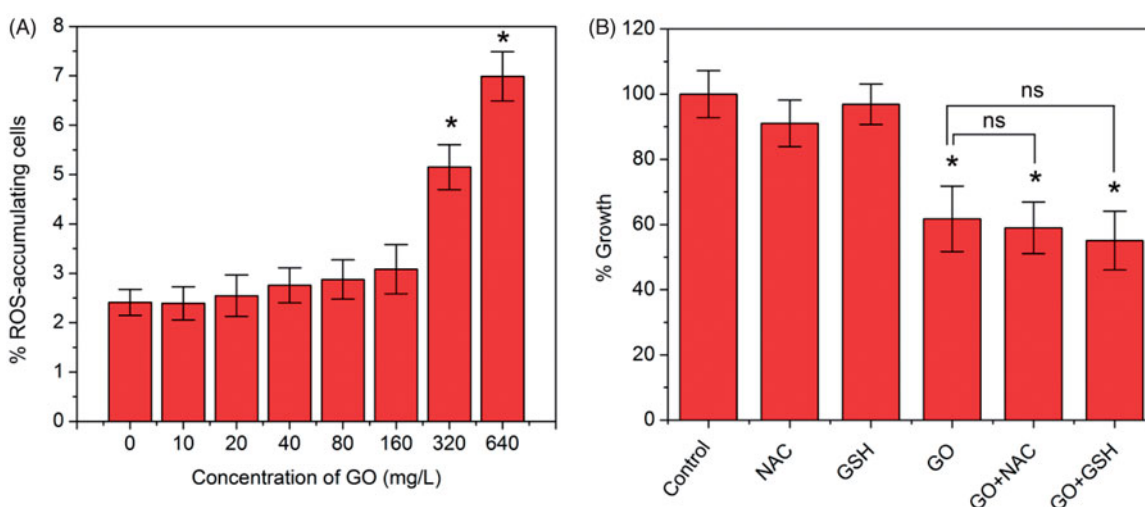


Figure 3. ROS accumulation does not contribute to GO-caused growth inhibition of yeast cells. (A) ROS levels in the GO-treated cells. Yeast cells were treated with GO at the indicated concentrations for 24 h, washed twice with PBS buffer, and stained with DCFH-DA. The stained cells were observed with a fluorescence microscope. The percent of DCF fluorescence-positive cells (ROS-accumulating cells) were calculated. (B) ROS scavenging. The yeast cells were cultured in the YPD medium or the medium containing 5 mM N-acetyl-L-cysteine (NAC), 5 mM glutathione (GSH), 160 mg/L GO, 160 mg/L GO plus 5 mM NAC, or 160 mg/L GO plus 5 mM GSH. After 24 h of incubation, the cells were counted. Values represent mean \pm SD. * indicates statistical difference between the treatment groups and the control group ($p < 0.05$). ns indicates that the difference is not significant.

inductively coupled plasma-mass spectrometry (ICP-MS) spectrometer (Elan drc-e, PekinElmer, Waltham, MA, USA).

Adsorption of Fe^{3+} to GO and rGO

To compare the adsorption affinity for Fe^{3+} between GO and rGO, a series of 40-mL amber glass vials were prepared, each containing 80 mg/L GO

(or rGO) and 28.5 mg/L Fe^{3+} (pH=6.5). The total volume was adjusted to 10 mL with double-distilled water. The vials were shaken at 60 rpm for 24 h to reach adsorption equilibrium. Afterward, the vials were centrifuged at 35,000 rpm for 60 min, and the supernatants were withdrawn to analyze the concentrations of un-adsorbed Fe^{3+} . The adsorbed mass was calculated based on a mass balance approach (Wang and Chen, 2005).

Statistical analysis

All the experiments were carried out in triplicate. Significant difference between the treatments was determined using one-way ANOVA ($p < 0.05$). Statistical analysis was carried out using Statistical Packages for the Social Sciences (SPSS, Version 20, Chicago, IL, USA).

Results and discussion

GO significantly inhibits growth of unicellular organisms at sublethal concentrations

Exposure of yeast cells to GO concentrations between 10 and 160 mg/L resulted in significant growth inhibition (Figure 2(A)). Exposure to GO at 10–20 mg/L caused a 20% decrease of biomass growth, whereas 160 mg/L of GO caused a 40% decrease. These GO concentrations are sublethal, since even at a GO concentration of 640 mg/L less than 1% of yeast cells were killed, as indicated by the PI staining data (Figure 2(B)). Similar results were observed with other unicellular organisms (i.e. the fungal pathogen *C. albicans*, the industrial fungus *K. pastoris*, and the common bacterium *P. fluorescens*), where exposure to GO at 160 mg/L did not result in noticeable cell death (Fig. S2) but exerted a significant inhibitory effect on cell growth (Fig. S3).

Common cytotoxicity mechanisms cannot explain the growth inhibition effects of GO

The commonly accepted cytotoxicity mechanisms of GO materials cannot explain the observed growth inhibition. For instance, membrane damage by the sharp edges of GO has been reported to cause GO toxicity to *Escherichia coli* and *Staphylococcus aureus* (Akhavan and Ghaderi, 2010; Gao et al., 2017b). However, PI staining showed that sublethal GO concentrations (≤ 160 mg/L) did not cause noticeable plasma membrane damage and related yeast cell death (Figure 2(B)). This may be attributed to differences in cell wall structure and composition among different microorganisms, which leads to different abilities to prevent GO from contacting and damaging the membrane. Apparently, the relatively thick yeast cell walls (Kollár et al., 1995) and exopolymeric layer of *P. fluorescens* (Quilès et al., 2012) hinder GO

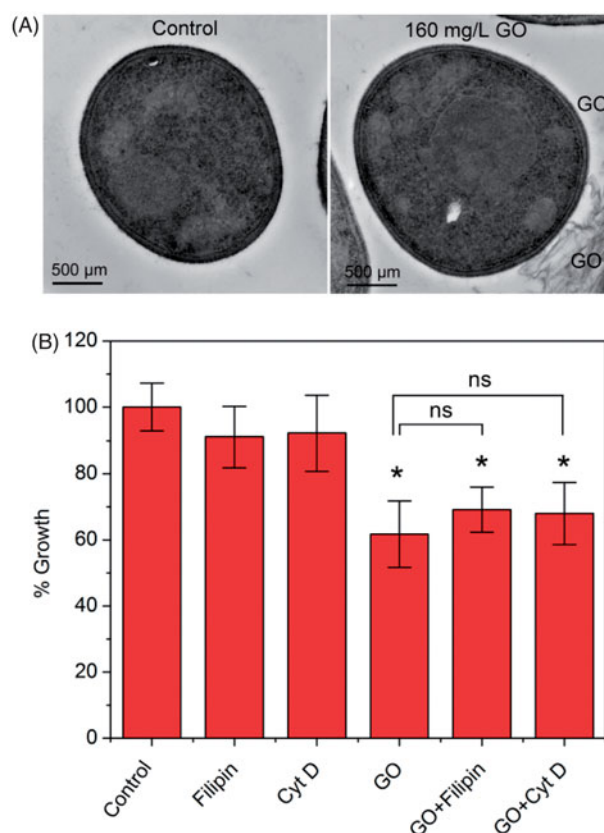


Figure 4. Endocytosis is not involved in GO-caused growth inhibition. (A) TEM observation of the control cells and the GO-treated cells. (B) Endocytosis inhibition. The yeast cells were cultured in the YPD medium or the medium containing 0.2 mg/L filipin, 2 μM Cyt D, 160 mg/L GO, 160 mg/L GO plus 0.2 mg/L filipin, or 160 mg/L GO plus 2 μM Cyt D. After cultured for 24 h, the cells in each group were counted, and % growth was calculated. Values represent mean \pm SD. * indicates significant difference between the treatment groups and the control group ($p < 0.05$). ns indicates that the difference is not significant.

penetration and mitigate contact with the plasma membrane. Previous studies have also shown that cytotoxicity of GO often involves ROS production and ROS-dependent cell damage (Li et al., 2014; Liu et al., 2011). However, DCFH-DA staining showed that GO at concentrations up to 160 mg/L had no impact on intracellular ROS levels; higher GO concentrations (320 and 640 mg/L) were required to do so (Figure 3(A)). Consistently, addition of ROS scavengers NAC and GSH could not relieve the inhibitory effect of GO on cell growth (Figure 3(B)). Consistently, no obvious plasma membrane damage or oxidative stress was observed following longer exposure (48 h) to sublethal concentrations (Fig. S4).

Nanoparticles uptake by various unicellular eukaryotic organisms commonly occurs via

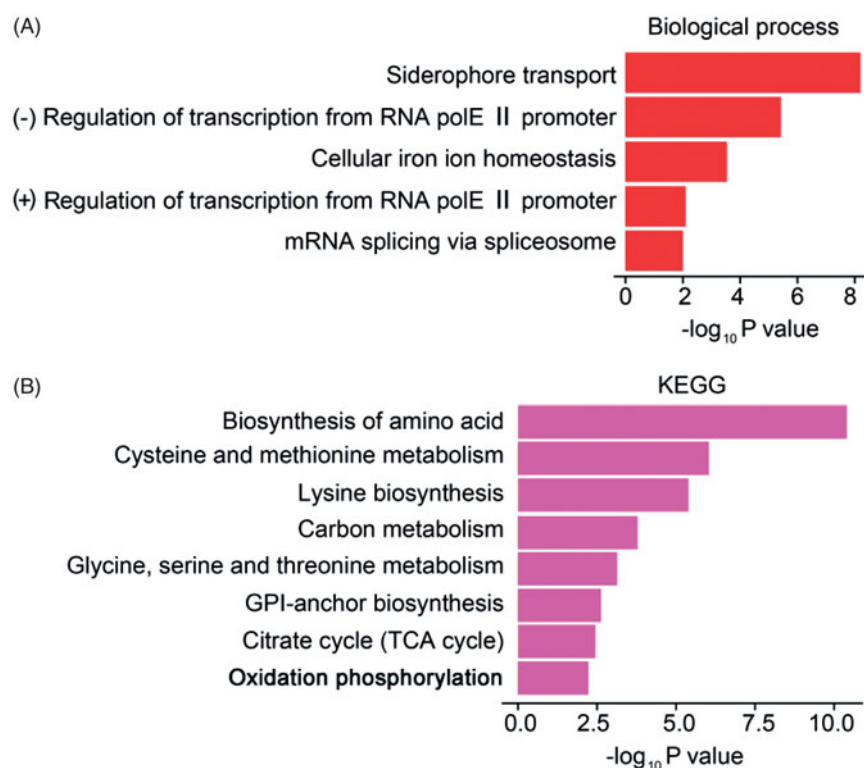


Figure 5. Biological process (BP) and KEGG analysis of the differentially expressed genes under GO treatment. (A) Up-regulated BP clusters in the cells treated by 160 mg/L GO for 24 h. + indicates positive; – indicates negative. (B) Down-regulated pathways in the GO-treated cells; the genes coding for these pathways are recorded in the Kyoto Encyclopedia of Genes and Genomes (KEGG). Note that all these metabolic processes require iron to maintain their activity.

endocytosis (Zou et al., 2016; Akhavan and Ghaderi, 2010; Maurer et al., 2016). To investigate the possible link between the observed growth inhibition exerted by GO and its endocytosis, we examined the distribution of GO in exposed yeast cells. TEM images show that GO mostly adhered to the cell wall, rather than entering into the cells (Figure 4(A)), indicating that the cell wall effectively prevented GO from internalization as previously reported (Lefevre et al., 2016). Similar to the cells receiving no GO treatments, the GO-treated cells had intact mitochondria, nuclei, and endomembrane systems (Figure 4(A)). Moreover, GO did not cause an obvious decrease of mitochondrial membrane potential (MMP) (Fig. S5A), and had no impact on mitochondrial morphology (Fig. S5B), corroborating that the mitochondria were not impaired by sublethal GO concentrations (160 mg/L). Furthermore, adding endocytosis inhibitors, filipin (inhibiting caveolae-associated endocytosis), and Cyt D (disrupting actin cytoskeleton dynamic) (Iversen, Skotland, and Sandvig, 2011), did not relieve GO-induced growth inhibition (Figure 4(B)).

Growth inhibition of GO is attributed to iron deficiency

The above results demonstrate that the inhibitory effect at sublethal GO concentrations is not due to well-known cytotoxicity mechanisms, and implicate interactions with extracellular (rather than intracellular) constituents. Since the main function of extracellular constituents in the culture medium is to supply nutrients for cell growth, we propose that GO likely hindered nutrient uptake and consequently resulted in the deficiency of essential nutrients. In response to a specific nutrient deficiency, cells generally upregulate genes associated with the uptake and metabolism of that nutrient (Fafournoux, Bruhat, and Jousse, 2000; Outten and Albetel, 2013; Puig, Askeland, and Thiele, 2005). Accordingly, mRNA sequencing and transcription profiling analysis were carried out to identify which nutrients were in deficiency for GO-treated cells.

Sublethal exposure to GO (160 mg/L) led to significant expression changes of 242 genes, including 97 up-regulated and 145 down-regulated genes (Fig. S6). Biological process (BP) analysis revealed

Table 1. Genes associated with iron metabolism that were up-regulated by GO treatment.

Systematic name	Gene name	Function
YEL065W	<i>SIT1</i>	Ferrioxamine B transporter; member of the ARN family of transporters that specifically recognize siderophore-iron chelates
YHL040C	<i>ARN1</i>	ARN family transporter for siderophore-iron chelates; responsible for uptake of iron bound to siderophores
YOR382W	<i>FIT2</i>	Facilitator of iron transport; involved in the retention of siderophore-iron in the cell wall
YOR383C	<i>FIT3</i>	Facilitator of iron transport; involved in the retention of siderophore-iron in the cell wall
YER145C	<i>FTR1</i>	High affinity iron permease
YMR058W	<i>FET3</i>	Multicopper oxidase that oxidizes ferrous (Fe^{2+}) to ferric iron (Fe^{3+}) for uptake by transmembrane permease Ftr1p
YOR384W	<i>FRE5</i>	Ferric reductase with similarity to Fre2p
YOL158C	<i>ENB1</i>	Endosomal ferric enterobactin transporter; expressed under conditions of iron deprivation
YLR205C	<i>HMX1</i>	ER localized heme oxygenase; involved in heme degradation during iron starvation and in the oxidative stress response
YLR136C	<i>TIS11</i>	mRNA-binding protein expressed during iron starvation; involved in iron homeostasis
YLR369W	<i>SSQ1</i>	Mitochondrial Hsp70-type molecular chaperone; required for assembly of iron/sulfur clusters into proteins

five up-regulated gene clusters. Three of these clusters were associated with general transcription regulation, and two clusters were associated with iron metabolism (i.e. siderophore transport and cellular iron ion homeostasis) (Figure 5(A)). These genes included *SIT1*, *ARN1*, *FIT2*, *FIT3*, *FTR1*, *FET3*, *FRE5*, *ENB1*, *HMX1*, *TIS11*, and *SSQ1*, encoding iron uptake-related transporters (*SIT1*, *ARN1*), facilitators (*FIT2*, *FIT3*), permease (*FTR1*), and oxidase/reductase (*FET3*, *FRE5*), as well as intracellular iron utilization factors (*ENB1*, *HMX1*, *TIS11*, and *SSQ1*) (Table 1). Up-regulation of these iron metabolism genes following exposure to sublethal GO concentrations was confirmed by RT-PCR (Fig. S7). Interestingly, up-regulation of genes associated with uptake of other nutrients was not observed. Therefore, we postulate that GO treatment caused iron deficiency.

During culturing of yeast cells in GO-free medium, the concentration of iron in the medium slightly decreased with increasing incubation time. After incubation for 24 h, the iron concentration decreased from 1.1 mg/L to 0.9 mg/L, indicating consumption of iron by cell growth (Figure 6(A)). Addition of GO—regardless of the presence of yeast cells—led to drastic decrease in the concentration of iron in the medium, to below 0.3 mg/L after 4 h of incubation and below 0.03 mg/L after 24 h (Figure 6(A)). Consistently, GO-treated cells had much lower intracellular iron concentrations than the control cells (Figure 6(B)). Therefore, GO caused a significant decrease of both extracellular and intracellular iron concentrations, indicating that iron sequestration by GO was a major inhibitory mechanism.

The possible connection between GO-caused iron depletion and growth inhibition was further investigated by addition of Fe^{3+} or the iron chelator BPS to the medium. Similar to the effect of GO, iron

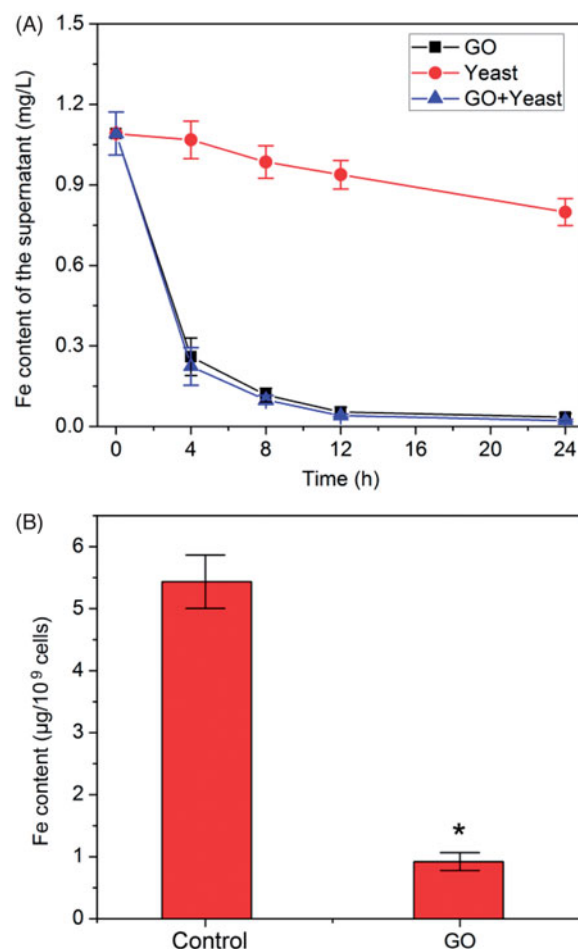


Figure 6. GO causes a significant decrease in iron concentration in both the medium (A) and yeast cells (B). (A) The YPD medium containing 160 mg/L GO, the medium containing yeast cells (the initial OD_{600} of 0.1) and the medium containing both 160 mg/L GO and yeast cells were incubated with shaking at 30 °C for 24 h. The suspensions were then centrifuged at 35,000 rpm to remove GO and yeast cells. Iron contents in the supernatants were detected by ICP-MS spectrometry. (B) The control cells and GO-treated yeast cells were washed several times with distilled water, digested with 33% HNO_3 and used for determination of iron contents. Values represent mean \pm SD. * indicates statistical difference between the GO treatment group and the control group ($p < 0.05$).

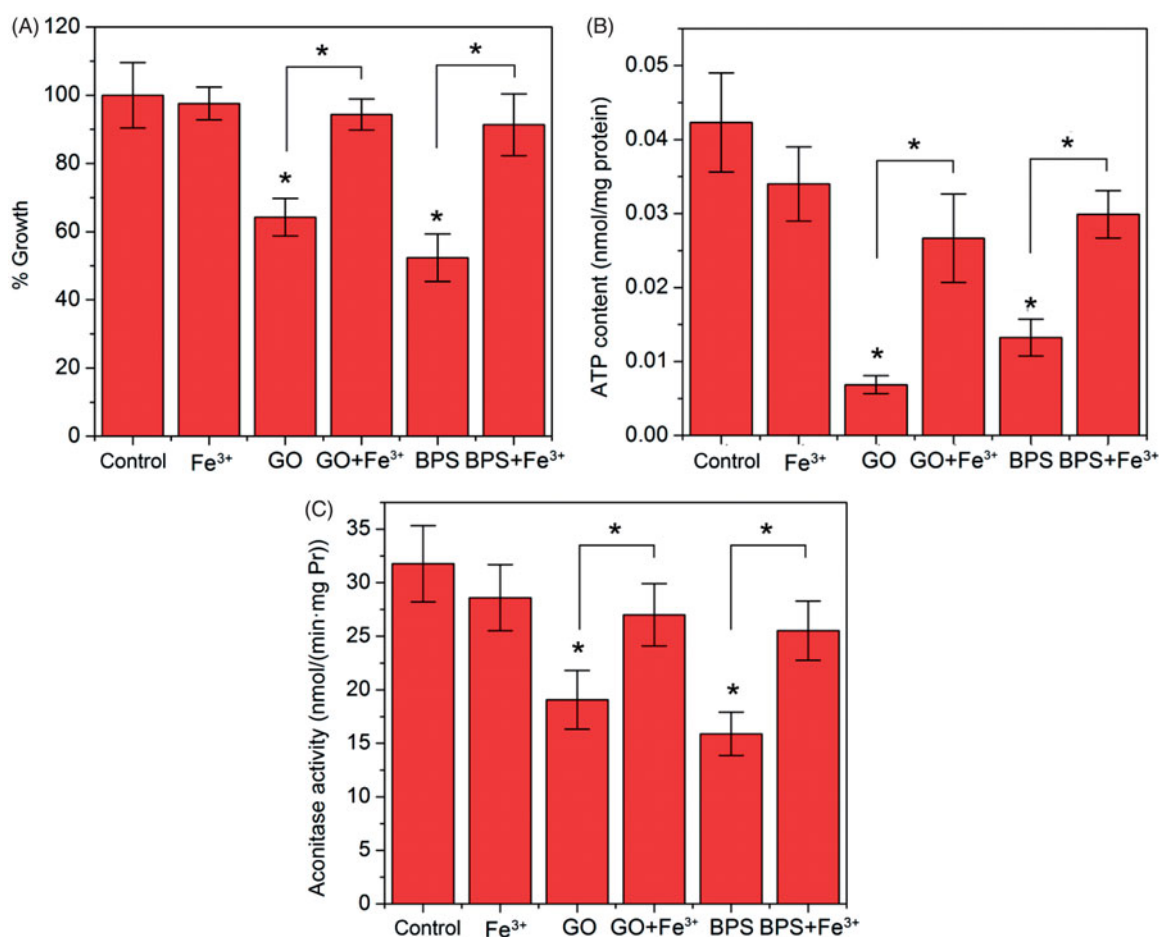


Figure 7. Iron addition restores yeast growth and iron-related functions. (A) Growth inhibition test. The yeast cells were cultured in YPD medium containing 1 mM Fe³⁺, 160 mg/L GO, 160 mg/L GO plus 1 mM Fe³⁺, 200 μ M BPS or 200 μ M BPS plus 1 mM Fe³⁺, and the percent of growth was determined. (B) ATP contents in the treated cells. (C) Aconitase activity. Values represent mean \pm SD. * indicates statistical difference among the treatments ($p < 0.05$).

sequestration by BPS significantly inhibited the growth of yeast cells (Figure 7(A)). While adding Fe³⁺ to the culture medium receiving no GO or BPS treatment had no effect on yeast growth, Fe³⁺ addition to the GO- or the BPS-amended medium restored yeast growth to the uninhibited level (Figure 7(A)). Similarly, Fe³⁺ addition also restored the growth of other tested organisms that had been inhibited by GO (Fig. S8).

XPS and FT-IR characterization of the GO surface showed the presence of oxygen-containing groups, including C–O, C=O and O–C=O (Figure 1(C,D)). We propose that these groups play a key role in adsorbing iron ions. To verify this, we compared the iron-binding capability between GO and rGO (with much lower abundance of surface O-functional groups). As expected, GO exhibited significantly greater adsorption affinity for Fe³⁺ than did rGO – the observed logarithm adsorption coefficient (log

K_d) values are 4.18–4.82 for GO, versus 2.76–2.98 for rGO. Neither GO nor did rGO cause noticeable cell damage at 160 mg/L (Fig. S9). However, unlike GO, rGO at this sublethal concentration did not significantly inhibit yeast cell growth (Fig. S10). Hence, reduction of GO attenuated both iron sequestration and growth inhibition, which corroborates the etiological relationship between iron deficiency and impaired growth, and demonstrates the critical role of O-functional groups on the GO surface.

GO-induced iron deficiency disrupts other iron-related physiological processes

Iron-containing cofactors (such as heme and iron-sulfur clusters) and mononuclear or di-iron enzymes are essential for most of the cellular metabolic processes (Lill and Mühlenhoff, 2008; Ozer and Bruick, 2007; Shakoury-Elizeh et al., 2010). For instance, ATP

production requires the participation of iron-containing cofactors, and iron depletion could affect ATP production. To assess this possibility, we determined ATP levels in cells amended with GO or BPS, both in the presence and absence of additional Fe^{3+} . While GO and BPS caused a drastic decrease of intracellular ATP levels, addition of Fe^{3+} significantly promoted ATP production in GO- or BPS-treated cells (Figure 7(B)), implying that inhibition of ATP production was caused by iron deficiency due to iron sequestration by GO.

Aconitase is an important enzyme in the tricarboxylic acid (TCA) cycle that converts citrate to isocitrate (Beinert and Kennedy, 1993; Regev-Rudzki et al., 2005). This enzyme contains the iron-sulfur cofactor, and hence its activity is regulated by intracellular iron levels (Pierik, Netz, and Lill, 2009). Similar to the ATP results, GO and BPS significantly hindered intracellular aconitase activity (and thus the TCA cycle), while Fe^{3+} addition recovered this activity in the GO- or BPS-treated cells (Figure 7(C)). In addition, GO downregulated other important pathways required for cell growth, such as oxidative phosphorylation and amino acid biosynthesis (Table S1, Figures 5(B) and S11), which might also contribute to iron deficiency-related growth inhibition.

Overall, GO-caused iron depletion contributes to dysfunction of iron cofactor-dependent enzymes and changes in gene expression that hinder metabolic activity and cell growth. Since most cancer cells and clinical pathogens, such as *C. albicans*, *Mycobacterium tuberculosis* and *Pseudomonas aeruginosa*, require iron for proliferation and invasion (Lounis et al., 2001; Ramanan and Wang, 2000; Renton and Jeitner, 1996; Richardson et al., 2009; Vasil and Ochsner, 1999), GO may be used as an iron scavenger for treating cancers and some microbial infections. However, caution should be exercised against some infections that are exacerbated by iron deficiency, such as production of diphtheria toxin by *Corynebacterium diphtheria*, where iron serves as a co-repressor of the *tox* gene (Schmitt and Holmes, 1991; Tao et al., 1994). In this case, GO-caused iron deficiency may enhance the virulence of this pathogen by promoting toxin production.

Conclusions

At sublethal concentrations, GO can significantly inhibit cell growth and metabolism. This inhibitory

effect is attributed to iron deficiency caused by the strong binding of iron to O-functional groups on the surface of GO. Extracellular iron sequestration disrupts several iron-related physiological processes and hinders metabolic activity. These findings highlight the importance to consider nutrient sequestration in assessing potential adverse effects of nanomaterials at sublethal concentrations, and encourage further research on potential biomedical applications of GO-based materials to treat iron-dependent diseases, such as cancers and some bacterial or fungal infections, by decreasing the bioavailable iron concentration.

Disclosure statement

No potential conflict of interest was reported by the authors.

Funding

This project was supported by the National Natural Science Foundation of China (Grants 21237002 and 31400132), the Ministry of Science and Technology of China (Grant 2014CB932001), and the National Science Fund for Distinguished Young Scholars (Grant 21425729). Partial funding was also provided by the NSF ERC on Nanotechnology-Enabled Water Treatment (EEC-1449500). The authors declare no competing financial interests.

References

- Akhavan, O., and E. Ghaderi. 2010. "Toxicity of Graphene and Graphene Oxide Nanowalls Against Bacteria." *ACS nano* 4: 5731–5736.
- Beinert, H., and M. C. Kennedy. 1993. "Aconitase, a Two-faced Protein: Enzyme and Iron Regulatory Factor." *FASEB journal: official publication of the federation of american societies for experimental biology* 7: 1442–1449.
- Beinert, H., M. C. Kennedy, and C. D. Stout. 1996. "Aconitase as Iron-sulfur Protein, Enzyme, and Iron-regulatory Protein." *Chemical reviews* 96: 2335–2374.
- Bianco, A. 2013. "Graphene: Safe or Toxic? The Two Faces of the Medal." *Angewandte chemie (International ed. in english)* 52: 4986–4997.
- Bulcke, F., K. Thiel, and R. Dringen. 2014. "Uptake and Toxicity of Copper Oxide Nanoparticles in Cultured Primary Brain Astrocytes." *Nanotoxicology* 8: 775–785.
- Buriak, J. M., and C. Toro. 2015. "Layer-by-layer Growth of Graphene Oxide-based Films for Electronics Applications in 1999: Early Leaders." *Chemistry of materials* 27: 1–2.
- Carpio, I. E. M., C. M. Santos, X. Wei, and D. F. Rodrigues. 2012. "Toxicity of a Polymer-graphene Oxide Composite Against Bacterial Planktonic Cells, Biofilms, and Mammalian Cells." *Nanoscale* 4: 4746–4756.

- Chatterjee, N., Y. H. Kim, J. Yang, C. P. Roca, S. W. Joo, and J. Choi. 2017. "A Systems Toxicology Approach Reveals the Wnt-MAPK Crosstalk Pathway Mediated Reproductive Failure in *Caenorhabditis elegans* Exposed to Graphene Oxide (GO) but Not to Reduced Graphene Oxide (rGO)." *Nanotoxicology* 11: 1–39.
- Chen, Y., X. Hu, J. Sun, and Q. Zhou. 2016. "Specific Nanotoxicity of Graphene Oxide During Zebrafish Embryogenesis." *Nanotoxicology* 10: 42–52.
- Chung, C., Y. K. Kim, D. Shin, S. R. Ryoo, B. H. Hong, and D. H. Min. 2013. "Biomedical Applications of Graphene and Graphene Oxide." *Accounts of chemical research* 46: 2211–2224.
- Compton, O. C., and S. T. Nguyen. 2010. "Graphene Oxide, Highly Reduced Graphene Oxide, and Graphene: Versatile Building Blocks for Carbon-based Materials." *Small (Weinheim an der bergstrasse, Germany)* 6: 711–723.
- Dreyer, D. R., S. Park, C. W. Bielawski, and R. S. Ruoff. 2010. "The Chemistry of Graphene Oxide." *Chemical society reviews* 39: 228–240.
- Ema, M., K. S. Hougaard, A. Kishimoto, and K. Honda. 2016. "Reproductive and Developmental Toxicity of Carbon-based Nanomaterials: a Literature Review." *Nanotoxicology* 10: 391–412.
- Fafournoux, P., A. Bruhat, and C. Jousse. 2000. "Amino Acid Regulation of Gene Expression." *The biochemical journal* 351: 1–12.
- Feng, M., H. Kang, Z. Yang, B. Luan, and R. Zhou. 2016. "Potential Disruption of Protein-protein Interactions by Graphene Oxide." *The journal of chemical physics* 144: 225102.
- Frost, R., S. Svedhem, C. Langhammer, and B. Kasemo. 2016. "Graphene Oxide and Lipid Membranes: Size-dependent Interactions." *Langmuir: The ACS journal of surfaces and colloids* 32: 2708–2717.
- Gao, Y., J. Wu, X. Ren, X. Tan, T. Hayat, A. Alsaedi, C. Cheng, and C. Chen. 2017b. "Impact of Graphene Oxide on the Antibacterial Activity of Antibiotics Against Bacteria." *Environmental science: Nano* 4: 1016–1024.
- Gao, Y., X. Ren, X. Tan, T. Hayat, A. Alsaedi, and C. Chen. 2017a. "Insights into Key Factors Controlling GO Stability in Natural Surface Waters." *Journal of hazardous materials* 335: 56–65.
- Gottschalk, F., T. Sun, and B. Nowack. 2013. "Environmental Concentrations of Engineered Nanomaterials: Review of Modeling and Analytical Studies." *Environmental pollution (Barking, Essex: 1987)* 181: 287–300.
- Gou, N., A. Onnis-Hayden, and A. Z. Gu. 2010. "Mechanistic Toxicity Assessment of Nanomaterials by Whole-cell-array Stress Genes Expression Analysis." *Environmental science & technology* 44: 5964–5970.
- Guo, L., A. Von Dem Bussche, M. Buechner, A. Yan, A. B. Kane, and R. H. Hurt. 2008. "Adsorption of Essential Micronutrients by Carbon Nanotubes and the Implications for Nanotoxicity Testing." *Small (Weinheim an der bergstrasse, Germany)* 4: 721–727.
- Hernandez-Viezcás, J. A., H. Castillo-Michel, J. R. Peralta-Videa, and J. L. Gardea-Torresdey. 2016. "Interactions Between CeO₂ Nanoparticles and the Desert Plant Mesquite: a Spectroscopy Approach." *ACS sustainable chemistry & engineering* 4: 1187–1192.
- Hoেকে, K. V., J. T. Quik, J. Mankiewicz-Boczek, K. A. D. Schamphelaere, A. Elsaesser, P. V. D. Meeren, and K. Rydzynski. 2009. "Fate and Effects of CeO₂ Nanoparticles in Aquatic Ecotoxicity Tests." *Environmental science & technology* 43: 4537–4546.
- Hummers, W. S., Jr, and R. E. Offeman. 1958. "Preparation of Graphitic Oxide." *Journal of the American chemical society* 80: 1339–1339.
- Iversen, T. G., T. Skotland, and K. Sandvig. 2011. "Endocytosis and Intracellular Transport of Nanoparticles: Present Knowledge and Need for Future Studies." *Nano today* 6: 176–185.
- Kiser, M. A., P. Westerhoff, T. Benn, Y. Wang, J. Perez-Rivera, and K. Hristovski. 2009. "Titanium Nanomaterial Removal and Release from Wastewater Treatment Plants." *Environmental science & technology* 43: 6757–6763.
- Kollár, R., E. Petráková, G. Ashwell, P. W. Robbins, and E. Cabib. 1995. "Architecture of the Yeast Cell Wall. The Linkage Between Chitin and Beta(1,3)-Glucan." *The journal of biological chemistry* 270: 1170–1178.
- Lefevre, E., N. Bossa, M. R. Wiesner, and C. K. Gunsch. 2016. "A Review of the Environmental Implications of In Situ Remediation by Nanoscale Zero Valent Iron (nZVI): Behavior, Transport and Impacts on Microbial Communities." *The science of the total environment* 565: 889–901.
- Li, J., G. Wang, H. Zhu, M. Zhang, X. Zheng, Z. Di, and X. Wang. 2014. "Antibacterial Activity of Large-area Monolayer Graphene Film Manipulated By Charge Transfer." *Scientific reports* 4: 4359.
- Liang, S., S. Xu, D. Zhang, J. He, and M. Chu. 2015. "Reproductive Toxicity of Nanoscale Graphene Oxide in Male Mice." *Nanotoxicology* 9: 92–105.
- Lill, R., and U. Mühlenhoff. 2008. "Maturation of Iron-sulfur Proteins in Eukaryotes: Mechanisms, Connected Processes, and Diseases." *Annual review of biochemistry* 77: 669–700.
- Liu, S., T. H. Zeng, M. Hofmann, E. Burcombe, J. Wei, R. Jiang, and Y. Chen. 2011. "Antibacterial Activity of Graphite, Graphite Oxide, Graphene Oxide, and Reduced Graphene Oxide: Membrane and Oxidative Stress." *ACS nano* 5: 6971–6980.
- Liu, W., Y. Wu, C. Wang, H. C. Li, T. Wang, C. Y. Liao, L. Cui, Q. F. Zhou, B. Yan, and G. B. Jiang. 2010. "Impact of Silver Nanoparticles on Human Cells: Effect of Particle Size." *Nanotoxicology* 4: 319–330.
- Lounis, N., C. Truffot-Pernot, J. Grosset, V. R. Gordeuk, and J. R. Boelaert. 2001. "Iron and *Mycobacterium tuberculosis* Infection." *Journal of clinical virology* 20: 123–126.
- Lowry, G. V., K. B. Gregory, S. C. Apte, and J. R. Lead. 2012. "Transformations of Nanomaterials in the Environment." *Environmental science & technology* 46: 6893–6899.

- Lundin, A. 1999. "Use of Firefly Luciferase in ATP-related Assays of Biomass, Enzymes, and Metabolites." *Methods in enzymology* 305: 346–370.
- Ma, C., Y. Rui, S. Liu, X. Li, B. Xing, and L. Liu. 2015. "Phytotoxic Mechanism of Nanoparticles: Destruction of Chloroplasts and Vascular Bundles and Alteration of Nutrient Absorption." *Scientific reports* 5: 11618.
- Mangadlao, J. D., C. M. Santos, M. J. L. Felipe, A. C. C. de Leon, D. F. Rodrigues, and R. C. Advincula. 2015. "On the Antibacterial Mechanism of Graphene Oxide (GO) Langmuir–Blodgett Films." *Chemical communications* 51: 2886–2889.
- Maurer, L. L., X. Yang, A. J. Schindler, R. K. Taggart, C. Jiang, H. Hsu-Kim, D. R. Sherwood, and J. N. Meyer. 2016. "Intracellular Trafficking Pathways in Silver Nanoparticle Uptake and Toxicity in *Caenorhabditis elegans*." *Nanotoxicology* 10: 831–835.
- Mueller, N. C., and B. Nowack. 2008. "Exposure Modeling of Engineered Nanoparticles in the Environment." *Environmental science & technology* 42: 4447–4453.
- Outten, C. E., and A. N. Albetel. 2013. "Iron Sensing and Regulation in *Saccharomyces cerevisiae*: Ironing Out the Mechanistic Details." *Current opinion in microbiology* 16: 662–668.
- Ozer, A., and R. K. Bruick. 2007. "Non-heme Dioxygenases: Cellular Sensors and Regulators Jelly Rolled into One?" *Nature chemical biology* 3: 144–153.
- Perreault, F., A. F. De Faria, S. Nejati, and M. Elimelech. 2015. "Antimicrobial Properties of Graphene Oxide Nanosheets: Why Size Matters." *ACS nano* 9: 7226–7236.
- Pierik, A. J., D. J. A. Netz, and R. Lill. 2009. "Analysis of Iron-sulfur Protein Maturation in Eukaryotes." *Nature protocols* 4: 753–766.
- Puig, S., E. Askeland, and D. J. Thiele. 2005. "Coordinated Remodeling of Cellular Metabolism During Iron Deficiency Through Targeted mRNA Degradation." *Cell* 120: 99–110.
- Qu, G., S. Liu, S. Zhang, L. Wang, X. Wang, B. B. Sun, N. Y. Yin, et al. 2013. "Graphene Oxide Induces Toll-like Receptor 4 (TLR4)-dependent Necrosis in Macrophages." *ACS nano* 7: 5732–5745.
- Quilès, F., P. Polyakov, F. Humbert, and G. Francius. 2012. "Production of Extracellular Glycogen by *Pseudomonas fluorescens*: Spectroscopic Evidence and Conformational Analysis by Biomolecular Recognition." *Biomacromolecules* 13: 2118–2127.
- Ramanan, N., and Y. Wang. 2000. "A High-affinity Iron Permease Essential for *Candida albicans* Virulence." *Science (New York, N.Y.)* 288: 1062–1064.
- Regev-Rudski, N., S. Karniely, N. N. Ben-Haim, and O. Pines. 2005. "Yeast Aconitase in Two Locations and Two Metabolic Pathways: Seeing Small Amounts is Believing." *Molecular biology of the cell* 16: 4163–4171.
- Ren, X., J. Li, X. Tan, W. Shi, C. Chen, D. Shao, T. Wen, et al. 2014. "Impact of Al_2O_3 on the Aggregation and Deposition of Graphene Oxide." *Environmental science & technology* 48: 5493–5500.
- Ren, X., Q. Wu, H. Xu, D. Shao, X. Tan, W. Shi, C. Chen, et al. 2016. "New insight into GO, Cadmium(II), Phosphate Interaction and its Role in GO Colloidal Behavior." *Environmental science & technology* 50: 9361–9369.
- Renton, F. J., and T. M. Jeitner. 1996. "Cell Cycle-dependent Inhibition of the Proliferation of Human Neural Tumor Cell Lines by Iron Chelators." *Biochemical pharmacology* 51: 1553–1561.
- Richardson, D. R., D. S. Kalinowski, S. Lau, P. J. Jansson, and D. B. Lovejoy. 2009. "Cancer Cell Iron Metabolism and the Development of Potent Iron Chelators as Anti-tumour Agents." *Biochimica et biophysica acta general subjects* 1790: 702–717.
- Ruiz, O. N., K. S. Fernando, B. Wang, N. A. Brown, P. G. Luo, N. D. McNamara, and C. E. Bunker. 2011. "Graphene Oxide: A Nonspecific Enhancer of Cellular Growth." *ACS nano* 5: 8100–8107.
- Schmitt, M. P., and R. K. Holmes. 1991. "Iron-dependent Regulation of Diphtheria Toxin and Siderophore Expression by the Cloned *Corynebacterium diphtheriae* Repressor Gene dtxR in *C. diphtheriae* C7 Strains." *Infection & immunity* 59: 1899–1904.
- Seabra, A. B., A. J. Paula, R. de Lima, O. L. Alves, and N. Duran. 2014. "Nanotoxicity of Graphene and Graphene Oxide." *Chemical research in toxicology* 27: 159–168.
- Shakoury-Elizeh, M., O. Protchenko, A. Berger, J. Cox, K. Gable, T. M. Dunn, and C. C. Philpott. 2010. "Metabolic Response to Iron Deficiency in *Saccharomyces cerevisiae*." *The journal of biological chemistry* 285: 14823–14833.
- Shen, J., Y. Hu, M. Shi, X. Lu, C. Qin, C. Li, and M. Ye. 2009. "Fast and Facile Preparation of Graphene Oxide and Reduced Graphene Oxide Nanoplatelets." *Chemistry of materials* 21: 3514–3520.
- Shirzadegan, M., P. Christie, and J. R. Seemann. 1991. "An Efficient Method for Isolation of RNA from Tissue Cultured Plant Cells." *Nucleic acids research* 19: 6055.
- Sitko, R., E. Turek, B. Zawisza, E. Malicka, E. Talik, J. Heimann, and R. Wrzalik. 2013. "Adsorption of Divalent Metal Ions from Aqueous Solutions Using Graphene Oxide." *Dalton transactions* 42: 5682–5689.
- Sun, Y., D. Shao, C. Chen, S. Yang, and X. Wang. 2013. "Highly Efficient Enrichment of Radionuclides on Graphene Oxide-supported Polyaniline." *Environmental science & technology* 47: 9904–9910.
- Tao, X., N. Schiering, H. Y. Zeng, D. Ringe, and J. R. Murphy. 1994. "Iron, DtxR, and the Regulation of Diphtheria Toxin Expression." *Molecular microbiology* 14: 191–197.
- Turco, R. F., M. Bischoff, Z. H. Tong, and L. Nies. 2011. "Environmental Implications of Nanomaterials: are We Studying the Right Thing?" *Current opinion in biotechnology* 22: 527–532.
- Valles, C., C. Drummond, H. Saadaoui, C. A. Furtado, M. He, O. Roubeau, L. Ortolani, M. Monthieux, and A. Penicaud. 2008. "Solutions of Negatively Charged Graphene Sheets and Ribbons." *Journal of the american chemical society* 130: 15802–15804.

- Vasil, M. L., and U. A. Ochsner. 1999. "The Response of *Pseudomonas aeruginosa* to Iron: Genetics, Biochemistry and Virulence." *Molecular microbiology* 34: 399–413.
- Waltman, R. J., J. Pacansky, and C. W. Bates. 1993. "X-ray Photoelectron Spectroscopic Studies on Organic Photoconductors Evaluation of Atomic Charges on Chlorodiane Blue and p-(diethylamino) Benzaldehyde Diphenylhydrazone." *Chemistry of materials* 5: 1799–1804.
- Wang, J., and B. L. Chen. 2005. "Adsorption and Coadsorption of Organic Pollutants and a Heavy Metal by Graphene Oxide and Reduced Graphene Materials." *Chemical engineering journal* 281: 379–388.
- Westerhoff, P., G. Song, K. Hristovski, and M. A. Kiser. 2011. "Occurrence and Removal of Titanium at Full Scale Wastewater Treatment Plants: Implications for TiO₂ Nanomaterials." *Journal of environmental monitoring: JEM* 13: 1195–1203.
- Wu, X., S. Tan, Y. Xing, Q. Pu, M. Wu, and J. X. Zhao. 2017. "Graphene Oxide as an Efficient Antimicrobial Nanomaterial for Eradicating Multi-drug Resistant Bacteria In Vitro and In Vivo." *Colloid surface B* 157: 1–9.
- Xu, N., Y. Dong, X. Cheng, Q. Yu, K. Qian, J. Mao, B. Zhang, and M. Li. 2014. "Cellular Iron Homeostasis Mediated by the Mrs4-Ccc1-Smf3 Pathway is Essential for Mitochondrial Function, Morphogenesis and Virulence in *Candida albicans*." *BBA molecular cell research* 1843: 629–639.
- Zhao, G., J. Li, X. Ren, C. Chen, and X. Wang. 2011. "Few-layered Graphene Oxide Nanosheets as Superior Sorbents for Heavy Metal Ion Pollution Management." *Environmental science & technology* 45: 10454–10462.
- Zhu, Y., S. Murali, W. Cai, X. Li, J. W. Suk, J. R. Potts, and R. S. Ruoff. 2010. "Graphene and Graphene Oxide: Synthesis, Properties, and Applications." *Advanced materials (Deerfield Beach, Fla.)* 22: 3906–3924.
- Zou, X., L. Zhang, Z. Wang, and Y. Luo. 2016. "Mechanisms of the Antimicrobial Activities of graphene materials." *Journal of the american chemical society* 138: 2064–2077.